VIII. Rotational Spectroscopy

1. Classification

The rotational spectra of molecules can be classified according to their "principal moments of inertia". Assume that the molecule rotates as a rigid body, that is, the relative nuclear positions are fixed. The moment of inertia I of any molecule about any axis through the center of mass is then given by

$$I = \sum_i M_i R_i^2 \tag{8.1}$$

where M_i and R_i are the mass and distance of atom i from the axis. One can always find one axis, called the c-axis, about which the moment of inertia has its *maximum* value, and another axis labelled the a-axis, about which I has its *minimum* value. It can be shown that the a and c axes must be mutally perpendicular. These, together with a third b-axis (perpendicular to both a and c), are called the "principal axes" of inertia and the corresponding moments of inertia I_a, I_b and I_c are the principal moments of inertia. Thus, according to convention:

$$I_c \geq I_b \geq I_a. \tag{8.2}$$

Mathematically, the principal axes are determined as follows: Recall that the center-of-mass position for a given axis may be found from the equation:

$$R_\alpha(C.M.) = \sum_i M_i R_i / \sum_i M_i \quad .$$

In general, for any rigid three dimensional body, there exists a 3×3 moment of inertia tensor. If we use any three axes defined by (xyz), the moment of inertia tensor has diagonal elements defined as $I_{xx} = \sum_i M_i(y_i^2 + z_i^2)$ (using the x-axis, for example), and off-diagonal elements given by $I_{xy} = -\sum_i M_i x_i y_i$, etc. (Note the minus sign in the off-diagonal terms). Clearly, the moment-of-inertia tensor is Hermetian, and so can be diagonalized to yield three (potentially) distinct eigenvalues that are the pinciple moments-of-inertia. The eigenvectors of the moments-of-inertia matrix in any coordinate system form the *direction cosines* that relate the arbitrary coordinate system to the principal axis coordinate system, that latter of which must rotate with the molecule.

Why do we care? If we use these principal axes, then the components of the rotational angular momentum $\mathbf{P}$ along these axes can be shown to be

$$P_a = I_a \omega_a \quad , \qquad P_b = I_b \omega_b \quad , \qquad P_c = I_c \omega_c \quad , \tag{8.3}$$

and the kinetic energy operator for a rigid-rotor simply becomes

$$T_{rot} = \frac{P_a^2}{2I_a} + \frac{P_b^2}{2I_b} + \frac{P_c^2}{2I_c}$$

In all other coordinate systems things are much more complicated!

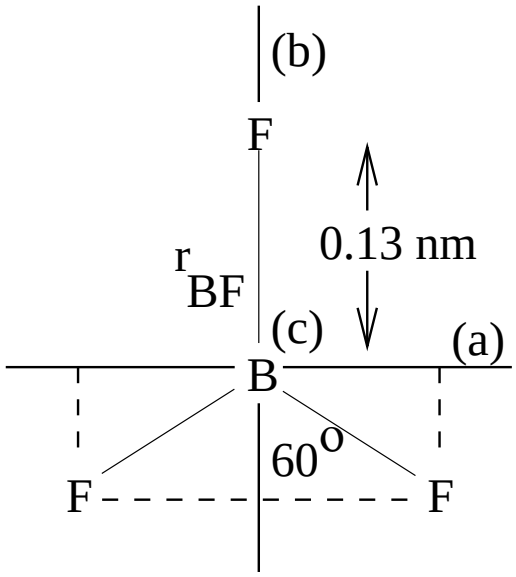

Figure 8.1– The structure and principal axes of boron trifluoride (BF_3).

As a simple example, let us calculate the moments-of-inertia for BF_3. This molecule is planar, with the three F atoms arranged around a central B atom at angles of 120° and a B-F distance of 1.30 Å. (See Figure 8.1). The center of mass is clearly at the B atom. One principal axis is perpendicular to the plane of the molecule, and since this axis will possess the largest moment of inertia, it is the c-axis. A second axis will pass through one of the B-F bonds, and the third will be mutually perpendicular to the first two.

For the c-axis, we find:

$$I_c = M_B \times 0.0 + 3M_F R_{BF}^2 = 3 \times 19(amu) \times (1.3\text{Å})^2 = 1.6 \times 10^{-38}\text{g cm}^2$$

For the other moments, we obtain:

$$I_a = M_B \times 0.0 + M_F R_{BF}^2 + 2M_F (R_{BF} sin30^\circ)^2 = 3/2\ M_F R_{BF}^2$$

$$I_a = M_B \times 0.0 + M_F \times 0.0 + 2M_F (R_{BF} sin60^\circ)^2 = 3/2\ M_F R_{BF}^2$$

Thus, we find $I_a = I_b = I_c/2$ for BF_3. This result is a consequence of the (numerous) symmetry properties of the molecule. For any planar molecule the c-axis is always perpendicular to the plane containing the nuclei, and in any coordinate system the moment-of-inertia tensor can be diagonalized simply by diagonalizing a 2×2 matrix. The direction cosines then simply collapse to a single rotation about the c-axis that brings the arbitrary axes into coincidence with the principal a, b-axes. For three-dimensional molecules the calculation of the moments and principal axes is straightforward, but tedious! (Not surprisingly, computer routines can now calculate the moment-of-inertia tensor for any molecule, and diagonalize it to obtain the principal axes and rotational constants).

Figure 8.2 illustrates the principal inertial axes for a number of molecules of different symmetry types. For a linear molecule such as HCN, one can easily see that

$$I_c = I_b > I_a = 0 \tag{8.4}$$

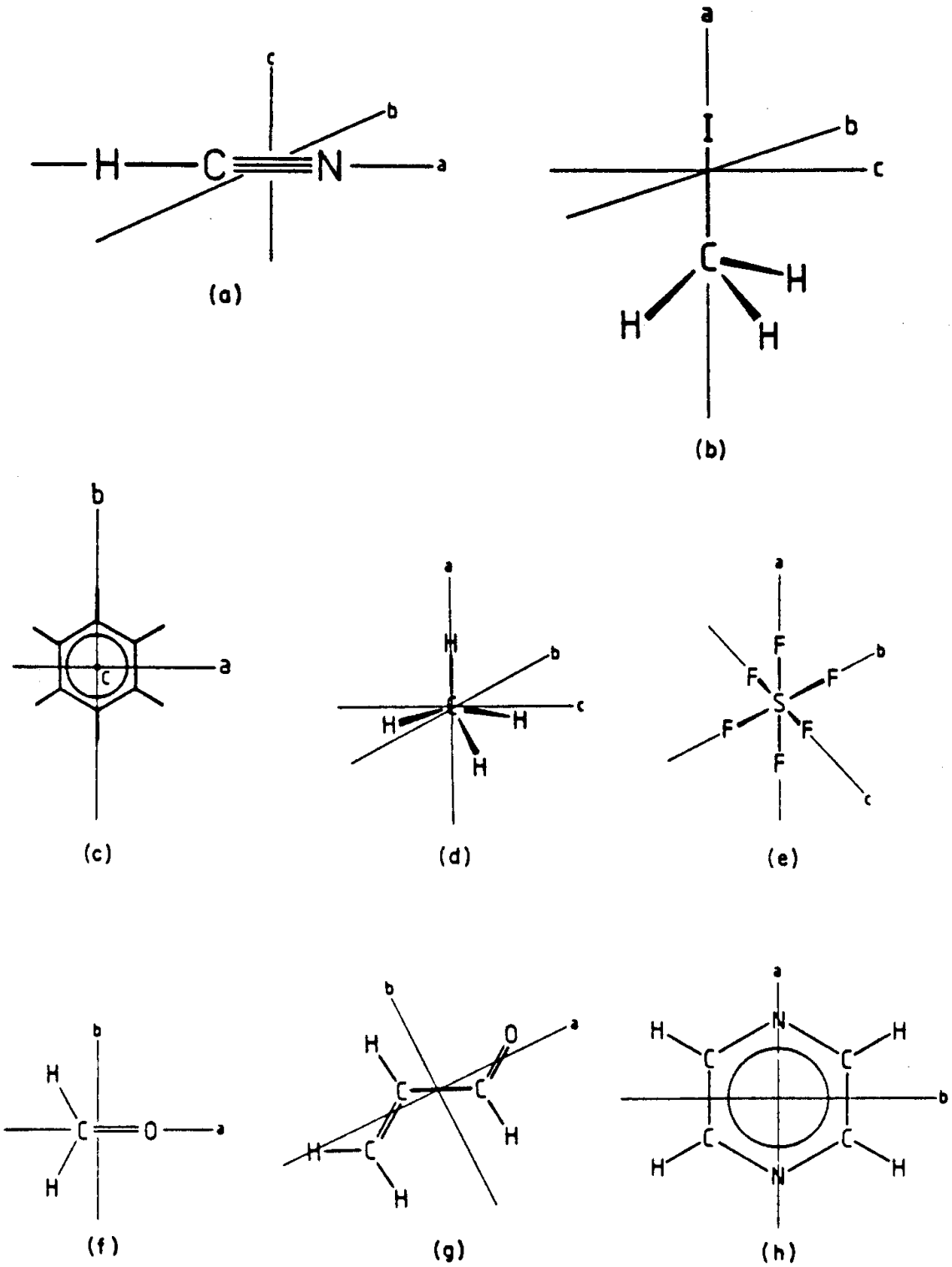

Figure 8.2– Principal inertial axes of (a) HCN, (b) methyl iodide, (c) benzene, (d) methane, (e) sulphur hexafluoride, (f) formaldehyde, (g) s-*trans*-acrolein, and (h) pyrazine.

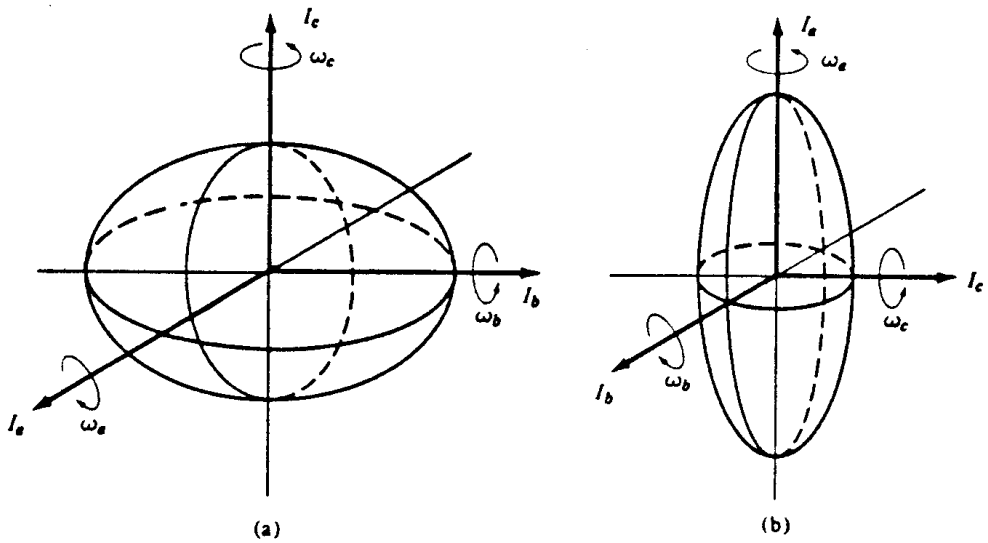

Figure 8.3– Principal axes for (a) oblate and (b) prolate symmetric tops.

where the b and c axes may be in any direction perpendicular to the internuclear a-axis. If the nuclei are taken to be point masses on the a axis, it is clear that I_a must be zero since all R_i in eq. (8.1) are zero. HCN is an example of a linear, symmetric rotor, and like BF_3, is a "symmetric top" molecule.

In general, for a symmetric top, two of the principal moments of inertia are equal and the third is non-zero. If

$$I_c = I_b > I_a \tag{8.5}$$

the molecule is a "prolate" symmetric top. A prolate top is the general shape of a football or a cigar (see Figure 8.3); molecular examples are methyl iodide (Figure 8.2b) and ammonia, NH_3. On the other hand, if

$$I_c > I_b = I_a, \tag{8.6}$$

we have an "oblate" symmetric top. Examples are a hockey puck, a frisbee, or in the case of molecules, benzene (Figure 8.2c).

A symmetric rotor always has a rotation axis C_n with n >2, which coincides with one of the principal axes of inertia, and two of the moments are always equal.

A special type of symmetric top occurs if

$$I_c = I_b = I_a \tag{8.7}$$

as in the case, for example, of CH_4 (methane) and SF_6 (Figure 8.2d and e). These are called "spherical top" molecules.

If the molecule possesses no C_n rotational symmetry axis with $n \geq 3$, all three principal moments of inertia are unequal,

$$I_c \neq I_b \neq I_a, \tag{8.8}$$

and the molecule is an "asymmetric top". Most molecules fall into this category. An example is formaldehyde, H_2CO, shown in Figure 8.2f.

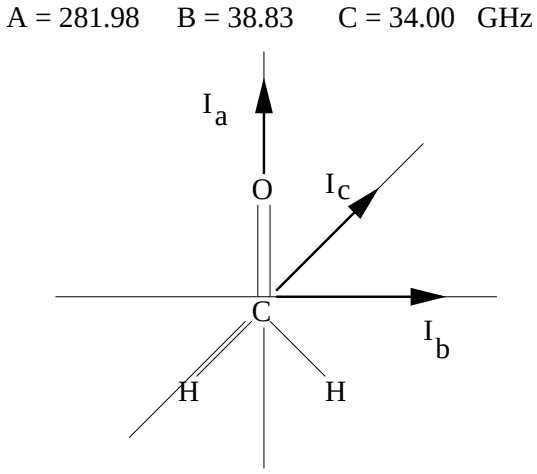

Figure 8.4– H_2CO as an example of a near prolate top. The two σ_v planes contain the A and B and A and C axes. The rotational constants lead to a Ray's asymmetry parameter of $\kappa = (2B - A - C)/(A - C) = -0.90$.

Although only a small fraction of all known molecules are true symmetric or spherical tops, there is more sizable group that falls into the category of "near-prolate" tops with

$$I_c \simeq I_b > I_a \tag{8.9}$$

or "near-oblate" tops with

$$I_c > I_b \simeq I_a. \tag{8.10}$$

Examples of near-prolate tops are C_{2v} molecules such as H_2O and H_2CO, and a molecule such as ethylene, C_2H_4. The convenience of classifying a molecule as a near-symmetric top will become evident soon.

2. Linear rotor

a) Energy expression

The energy levels of a linear rotor have already been given in section VII.

$$F(J) \quad = \quad BJ(J+1) \tag{8.11}$$

where the rotational constant $B = 1/2\ \mu R^2$ or $B = h/8\pi^2 c\mu R^2$ if B is expressed in cm^{-1} and the inertial moment $I = \mu R^2$ is in g·cm^2.

More generally, with centrifugal distortion terms the rotational energies are:

$$F_v(J) \quad = \quad B_v J(J+1) \ - \ D_v J^2(J+1)^2 \ + \ ... \tag{8.12}$$

b) Selection rules

Just as for atoms, the transition probabilities for electric dipole radiation are proportional to the square of the transition moment

$$R = < \Psi_u^{tot} | \vec{d} | \Psi_l^{tot} >, \tag{8.13}$$

where the dipole moment operator

$$\vec{d} \;=\; \vec{d}^{el} \;+\; \vec{d}^{nuc} \;=\; -\sum_i \vec{r}_i \;+\; \sum_\alpha Z_\alpha \vec{R}_\alpha. \tag{8.14}$$

In the Born-Oppenheimer approximation, R becomes:

$$R \;=\; < \Psi_u^{el}\Psi_u^{vib}\Psi_u^{rot}|\vec{d}^{el} + \vec{d}^{nuc}| < \Psi_l^{el}\Psi_l^{vib}\Psi_l^{rot} > \tag{8.15}$$

$$\equiv < e'v'J'|\vec{d}^{el} + \vec{d}^{nuc}|e''v''j'' >$$

where the integration in (8.15) is over the coordinate space of both the electrons and the nuclei. For *pure* rotational transitions, $e' = e''$ and $v' = v''$, so that we obtain:

$$R \;=\; < v''J' < e''|\vec{d}^{el} + \vec{d}^{nuc}|e'' > v''J'' > \tag{8.16}$$

where

$$\mu(R) \;=\; < e''(\vec{R})|\vec{d}^{el} + \vec{d}^{nuc}|e''(\vec{R}) > \tag{8.17}$$

is the permanent dipole moment of the electronic state. Thus, we see that the electric dipole transition matrix element (8.16) is only non-zero if $\vec{\mu}(R)$ is non-zero. In addition, we obtain the usual requirement from the angular part that $J' = J'' \pm 1$ (if $J' = J''$ there is no transition). Thus, the selection rules for pure rotational transitions are:

1. The molecule must have a permanent dipole moment.
2. $\Delta J \equiv J' - J'' = \pm\, 1$.

The first selection rule implies that pure rotational transitions in "homonuclear" diatomic molecules such as H_2, C_2, O_2 and N_2, or symmetric linear polyatomics like CO_2 and H-C≡C-H (acetylene), etc... are E1 forbidden, but that they are allowed in "heteronuclear" diatomics, such as CO, NO, OH, SiO, and even HD (for which the dipole moment is only 5.9×10^{-4} Debye) and other linear polyatomics like HCN and HC_3N. Typically, dipole moments are about 1-2 D, although that of CO happens to be comparatively small, only 0.11 Debye, due to a coincidental near-cancellation of opposing contributions in its complicated electronic structure.

Selection rule #2 implies that the transitions can occur only between *adjacent* rotational levels, so that ΔJ=1 in all cases (both in absorption and emission). This leads to the regularly spaced spectra such as shown schematically in Figure 7.4. Since the transition probabilities vary little with J, the relative intensities of the lines are proportional to the populations in the various levels, which, in turn, are governed by a Boltzmann distribution at the temperature T of the gas. Because the rotational levels lie close in energy, several levels can be populated significantly, even at the low temperatures in interstellar clouds. For example, for CO, the energy spacing between the J=0 and 1 levels corresponds to only 5.5 K. The spectrum will therefore at high temperatures, T≥100 K, have the appearance as shown in Figure 8.5. A useful rule of thumb is that the rotational quantum number corresponding to the most intense line J_{max} is the integer nearest to $0.59[\mathrm{T(K)/B(cm^{-1})}]^{1/2}$ and the frequency of the band envelope maximum, measured relative to the band origin, is $\tilde{\nu}_{max}(\mathrm{cm}^{-1}) \approx 1.18(\mathrm{BT})^{1/2}$.

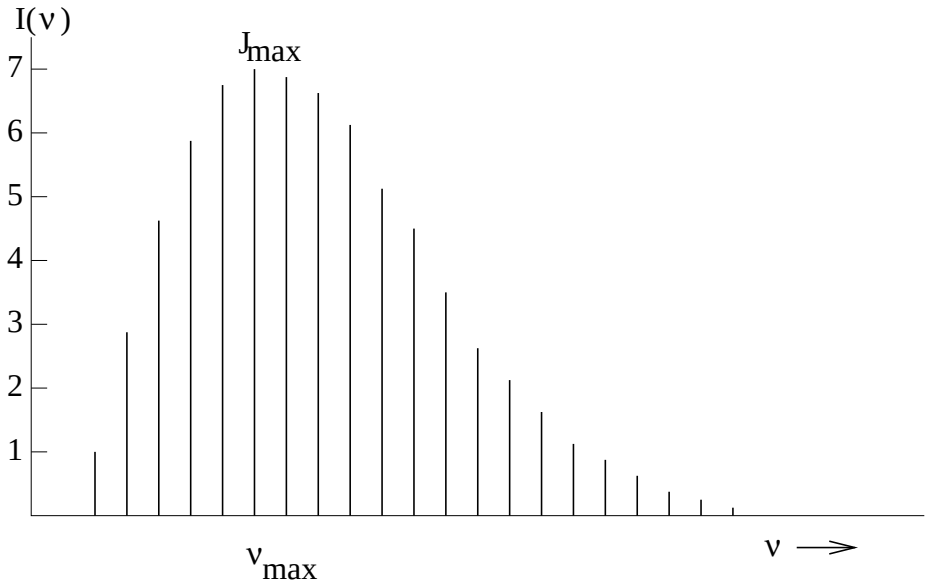

Figure 8.5– Typical rotational absorption band contour, for T/B approximately equal to 70 (for example, NO at 120K, or HCl at 740K).

Note that the rotational wave functions change sign under reflection of all particles through the origin for odd J, but that they are unchanged for even J. Thus, the even-J functions have + parity, whereas the odd-J functions have – parity.

c) Nuclear spin statistics.

As we have seen in §I, part 5e some nuclei have a non-zero nuclear spin I. This can be included in the total wavefunction of the molecule by adding a part Ψ^{ns}:

$$\Psi = \Psi^{el}\Psi^{vib}\Psi^{rot}\Psi^{ns} \tag{8.18}$$

where Ψ^{ns} depends only on the nuclear spin coordinates. In this section, we are concerned only with the symmetry properties of Ψ^{rot} and Ψ^{ns}.

If the molecule is symmetrical (for example, H_2, H-C≡C-H,...) restrictions may apply to the nuclear spin states, because of the identical nuclei. As we saw earlier, the wave function for a system of electrons must be antisymmetric with respect to exchange of any two electrons in the system. This is a property not only of electrons, but of any particle with half-integral spin, including many nuclei. Such particles are said to obey "Fermi-Dirac statistics". Particles with integral (including 0) spin possess wave functions that must be symmetric with respect to exchange of any two (indistinguishable) particles, and obey "Bose-Einstein statistics". Table 8.1 lists a number of important nuclei, their I, and their statistics.

Let us now consider the consequences of these rules in the simple case of $^1H_2$. In this molecule, both Ψ^{el} for the ground electronic state X $^1\Sigma_g^+$, and Ψ^{vib} are symmetric to nuclear exchange, irrespective of the value of v. Since I=1/2 for ^{1}H, Ψ, and therefore $\Psi^{rot}\Psi^{ns}$, must be antisymmetirc to nuclear exchange. It can be shown that for even values of J, Ψ^{rot} is symmetric (s) to exchange, and for odd J, Ψ^{rot} is antisymmetric (a) to exchange, as noted above.

Table 7.1

Nucleus	Protons	Neutrons	Spin I	Statistics[a]
H	1	0	1/2	FD
D	1	1	1	BE
T	1	2	1/2	FD
^{3}He	2	1	1/2	FD
^{4}He	2	2	0	BE
^{12}C	6	6	0	BE
^{13}C	6	7	1/2	FD
^{14}N	7	7	1	BE
^{15}N	7	8	1/2	FD
^{16}O	8	8	0	BE
^{17}O	8	9	5/2	FD
^{18}O	8	10	0	BE
^{19}F	9	10	1/2	FD
^{127}I	53	74	5/2	FD

[a] Key: FD = Fermi-Dirac; BE = Bose-Einstein

What are the possible nuclear spin states? Just as for the case of 2 electrons (see p.21), the spins I=1/2 of the two ^{1}H nuclei can be combined to a triplet and a singlet function:

$$\text{(s)} \quad \Psi^{ns} = \begin{cases} \alpha(1)\alpha(2) \\ \sqrt{\frac{1}{2}}[\alpha(1)\beta(2)+\beta(1)\alpha(2)] \\ \beta(1)\beta(2) \end{cases} \tag{8.19a}$$

$$\text{(s)} \quad \Psi^{ns} = \sqrt{\frac{1}{2}}[\alpha(1)\beta(2)-\beta(1)\alpha(2)] \tag{8.19b}$$

Clearly, (8.19a) is symmetric to nuclear exchange, whereas (8.19b) is antisymmetric. In general, for a homonuclear diatomic molecule there are $(2I+1)(I+1)$ symmetric and $(2I+1)I$ antisymmetric nuclear spin wave functions so that

$$\frac{\text{Number of (s) functions}}{\text{Number of (a) functions}} = \frac{I+1}{I}. \tag{8.20}$$

In order that $\Psi^{rot}\Psi^{ns}$ is always antisymmetric for $^1H_2$, only antisymmetric Ψ^{ns} functions can be associated with even J states, and only symmetric Ψ^{ns} with odd J states. Interchange between states with Ψ^{ns} symmetric and antisymmetric can only occur through collisions in which a nucleus is exchanged, so that $^1H_2$ can be regarded as consisting of two distinct forms:

1. '*para*'-hydrogen with Ψ^{ns} antisymmetric, so that the nuclear spins are antiparallel
2. '*ortho*'-hydrogen with Ψ^{ns} symmetric, so that the nuclear spins are parallel.

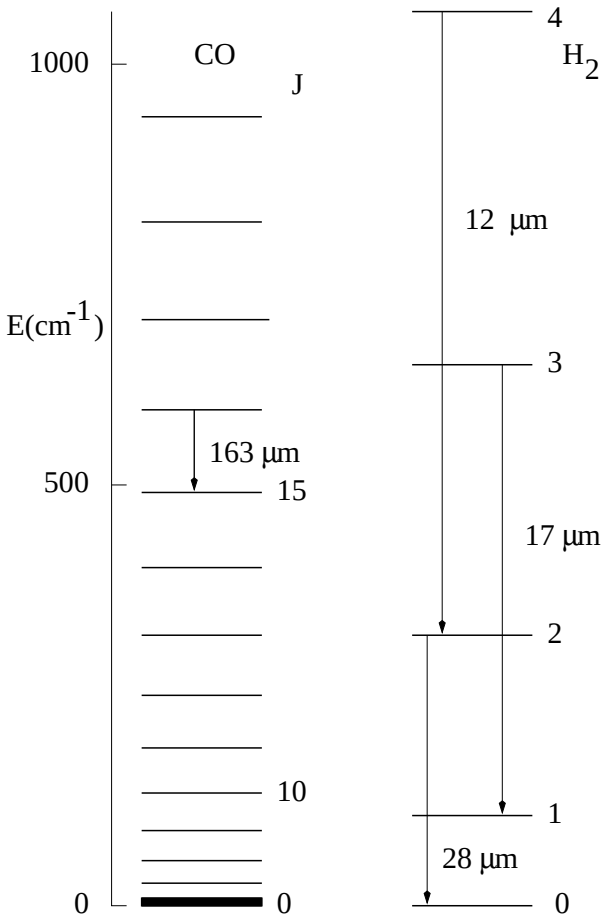

Figure 8.6– Rotational ladders for CO and H_2.

Thus, *para*-H_2 can exist only in even J states, and *ortho*-H_2 in odd J states. Table 8.2 summarizes the possible states of H_2, whereas Figure 8.6 illustrates the energy levels and compares the spacing with that of a heavy rotor such as CO. At high temperatures (T$\geq$1000 K), there is appreciable population in the higher J levels, and so *ortho*-$H_2 \approx$ *para*-H_2. When the temperature is low (T<100 K), however, only the J=0 contains significant population, so that H_2 is mostly in the *para*-form.

Table 8.2 – Nuclear spin statistics of $^1H_2$

J	parity	s/a	Nucl. spin states	Tot. stat. wt.*	E(K)
0	+	s	1	1	0.0
1	–	a	3	9	170.5
2	+	s	1	5	509.9
3	–	a	3	21	1015.1
4	+	s	1	9	1681.7

* Total statistical weight = $g_N(2J+1)$

Radiative transitions can occur only through the electric quadupole operator with $\Delta J = 2$. The longest wavelength pure rotational transition $J = 2 \rightarrow 0$ occurs at 28.21 μm, whereas the $J = 3 \rightarrow 1$ transition appears at 17.03 μm.

All other homonuclear diatomic molecules with $I = 1/2$ for each nucleus, such as $^{19}F_2$, also have *ortho* and *para* forms with odd and even J, and nuclear spin statistical weights of 3 and 1, respectively. Also, for a symmetric linear polyatomic molecule like acetylene ^{1}H^{12}-C$\equiv^{12}$C-^{1}H the situation is very similar to H_2 since I=0 for ^{12}C. The main difference is that the rotational energy levels are much more closely spaced, so that only at very low temperature, is C_2H_2 predominantly in the *para* form.

If I=1 for each nucleus, as in D_2 or $^{14}N_2$, the total wavefunction must be symmetric to nuclear exchange. The two $I = 1$ spins give rise to 9 nuclear spin functions of which 6 are symmetric (*ortho*), and 3 antisymmetric (*para*) to exchange. Thus, for D_2 (or $^{14}N_2$) the *ortho* form can have only even J, and the *para* form only odd J. At high temperatures, there is roughly twice as much of the *ortho* as the *para* form. At low temperatures, the excess of the ortho form is even larger.

For $^{12}C_2$ and $^{16}O_2$, I=0 for each nucleus, so that the total wave function must again be symmetric to nuclear exchange. Consider first the case of $^{12}C_2$. The ground electronic state, X $^1\Sigma_g^+$, has (s) symmetry, so that we again have to consider the symmetry of the product $\Psi^{rot}\Psi^{ns}$. Because I=0, Ψ^{ns}=1, and the symmetry is determined by Ψ^{rot}. Since only symmetric functions are permitted, this means that $^{12}C_2$ can have *only even* J levels; all states with odd J are 'missing'! (The levels simply do not exist at all!)

For $^{16}O_2$, the case is reversed, since the ground state wave function, $^3\Sigma_g^-$, has (a) symmetry. Thus, $^{16}O_2$ has *only odd* J levels, and all states with even J are missing. Note that the same holds for $^{18}O_2$, but not, for example, for ^{16}O^{17}O or ^{16}O^{18}O. Thus, in a spectrum of oxygen with natural isotopic ratios, lines with even J will appear very weakly due to the asymmetrical isotopes ^{16}O^{18}O, etc....

d) Higher order terms

Recall that Λ is the quantum number of angular momentum of the electrons about the internuclear axis. The component of the total angular momentum perpendicular to the internuclear axis is $\vec{N}$, and it represents essentially the rotation of the nuclei alone. When Λ=0, the total angular momentum $\vec{J}$ is perpendicular to the internuclear axis, and $\vec{J}$=$\vec{N}$. When $\Lambda \neq$0, the whole system still rotates about $\vec{J}$ with the same frequency as a simple rotor having the I and J. Allowed values of J in this general case are

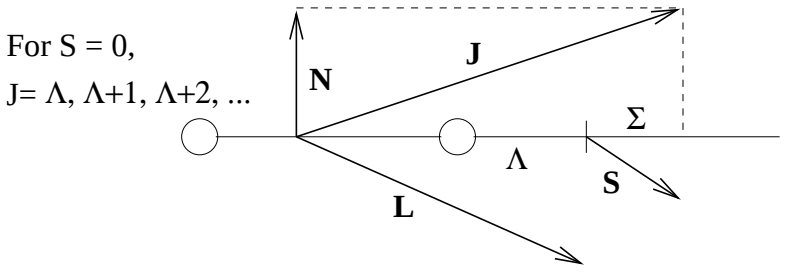

Also, we have seen that when $\Lambda > 0$, the states are two-fold degenerate because for a given $\vec{N}$ and for each value of J, there are two directions of Λ.

Λ-doubling

The degeneracy of the Λ levels can be lifted by coupling between the electronic motion and nuclear rotation: this is known as Λ-doubling of rotational levels.

For a linear rotor, the energy levels are given by

$$F_v(J) = B_v J(J+1) + (A_v - B_v)\Lambda^2 \tag{8.21}$$

where $A = h/8\pi^2 cI_A >> B$. The constant A arises from the fact that the moment of inertia about the internuclear axis a is not exactly zero, if several electrons are distributed about the two nuclei.

However, A is nearly constant for a given electronic state: thus the term $A\Lambda^2$ is just a constant shift in the rotational levels and can be ignored to first order in discussing the level spacings:

$$F_v(J) \simeq B_v[J(J+1) - \Lambda^2]. \tag{8.22}$$

In the simplest case of a $^1\Pi$ state, there is an additional splitting that arises from the coupling of B and Λ, given by:

$$\Delta\nu = qJ(J+1). \tag{8.23}$$

Although one can say that this so-called Λ-doubling arises from the interaction of nuclear rotation and electronic motion, describing that interaction quantitatively is more difficult. In fact, it is typically more useful to view it in terms of the interaction of two different electronic states with different electronic angular momenta (that is, different values of Λ): for example, the splitting in $^1\Pi$ rotational levels can be described quantitatively as a perturbation that arises due to a nearby $^1\Sigma$ state.

(ii) Spin-orbit interaction

As for atoms, electron spin causes further complications via the spin-orbit interaction. First, in the absence of rotation, multiplet-sigma states $^2\Sigma$, $^3\Sigma$, ... are unsplit, but multiplet-pi $^2\Pi$,$^3\,\Pi$,... and multiplet-delta $^2\Delta$,$^3\,\Delta$,... states are split into $2S$+1 components labelled with a quantum number

$$\Sigma = S, S-1, ... -S.$$

The combinations of spin angular momentum and electronic orbital momentum along the axis are labelled by a quantum number

$$\Omega = \Lambda + \Sigma \tag{8.24}$$

which is often indicated as a subscript following the term symbol.

Examples:

$^2\Pi: \quad 2S+1 = 2 \quad \Rightarrow \quad \Sigma = -1/2, 1/2 \quad , \quad \Lambda = 1 \quad \Rightarrow \quad \Omega = 1/2, 3/2.$

Thus there are $^2\Pi_{1/2}$ and $^2\Pi_{3/2}$ states possible, each of which has its own complement of rotational levels, each of which is split by $\Lambda - doubling$. An example is provided by the OH molecule, which will be discussed later.

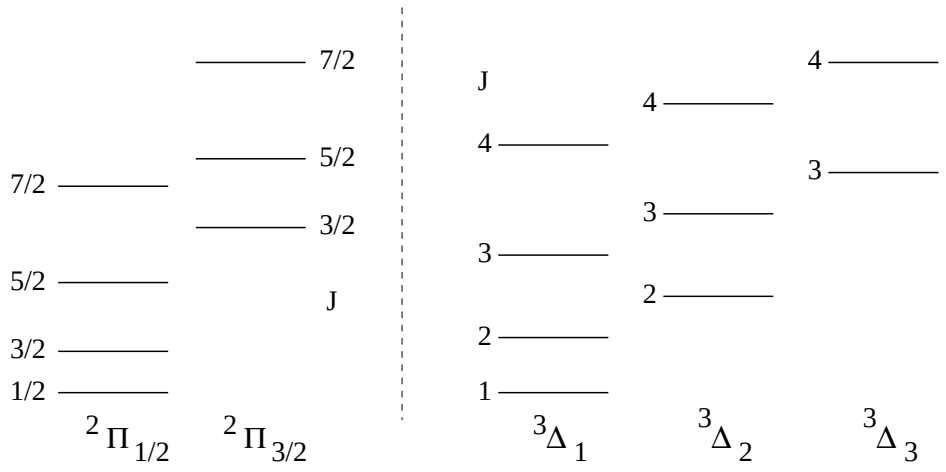

Figure 8.7– The spin-orbit interaction in $^2\Pi$ and $^3\Delta$ rotors.

$^3\Pi$ $2S+1=3 \Rightarrow \Sigma=-1,0,+1$, $\Lambda=1 \Rightarrow \Omega=0,1,2.$

Thus, there are $^3\Pi_0$,$^3\Pi_1$ and $^3\Pi_2$ states.

The next complication is the coupling of spin and rotation. For a $^1\Sigma$ state there is, of course, nothing to do! The general case for other states is intermediate coupling, but many states can be described, at least in a first approximation, as belonging to limiting c ases first catalogued by Hund and referred to as Hund's coupling cases. (This is somewhat analogous to the LS and jj coupling schemes for atoms.)

Hund's case (a): Here the electronic spin-orbit coupling $A\vec{L}\cdot\vec{S}$ is large, but the nuclear rotation-electron coupling $\vec{N}\cdot\vec{L}$ is small. Thus Ω remains a 'good' quantum number, and the energy expression becomes:

$$F(J) \simeq B_v[J(J+1)-\Omega^2] \tag{8.25}$$

(see Figure 8.7). Note that each Ω state has its own rotational ladder.

Hund's case (b): In this case, the electronic spin-orbit coupling is small, so the spin couples to the axis of rotation of the molecule. This situation almost always applies to Σ states where Λ=0; it often applies to Π and Σ states in light molecules. If $\vec{N}$ is the total angular momentum, excluding spin, the component Λ on the axis, then:

$$\vec{J}=\vec{N}+\vec{S} \tag{8.26}$$

that is, $J=N+S, N+S-1, ...|N-S|$ levels with the same N are close together. For example, in a $^2\Sigma$ state, the energy levels are:

$$F_1(N)=B_vN(N+1)+1/2\gamma N \tag{8.27a}$$

$$F_2(N)=B_vN(N+1)-1/2\gamma(N+1) \tag{8.27b}$$

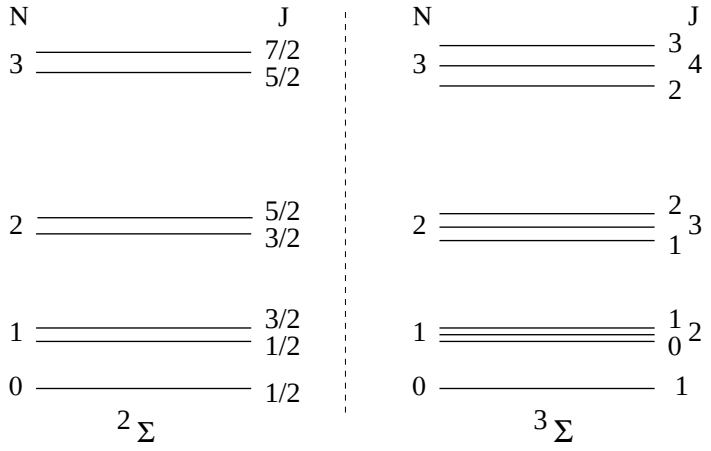

Figure 8.8– Illustration of the energy levels for $^2\Sigma$ and $^3\Sigma$ molecules.

where γ is the spin-rotation constant. For example, in MgH, B_0=5.7365 cm^{-1} while γ_0=0.0264 cm^{-1}.

General approximate expressions for the energy levels for molecules near one or the other of these limiting cases, and for intermediate coupling cases, can be found, for example, in G. Herzberg, Spectra of Diatomic Molecules, Chapter 5. The selection rules for these transitions are in general $\Delta J = 0, \pm 1$ and parity must change $+ \leftrightarrow -$ for E_1 transitions.

As for atoms, hyperfine splittings occur in the energy levels if the nuclei have non-zero nuclear spins. The total angular momentum i nthis case is

$$\vec{F} = \vec{J} + \vec{I}_1 + \vec{I}_2. \tag{8.28}$$

Since such nuclei possess electric quadrupole as well as spin magnetic moments, the hyperfine energy expression must include both of these interactions. Hyperfine splittings are readily observed in the rotational spectra of molecules in cold interstellar clouds, and can provide excellent clues regarding the identity of the molecule. Figure 8.9 illustrates the hyperfine structure splitting for the CN molecule, and the accompanying figure shows the observed spectra toward Orion. The hyperfine components are clearly seen.

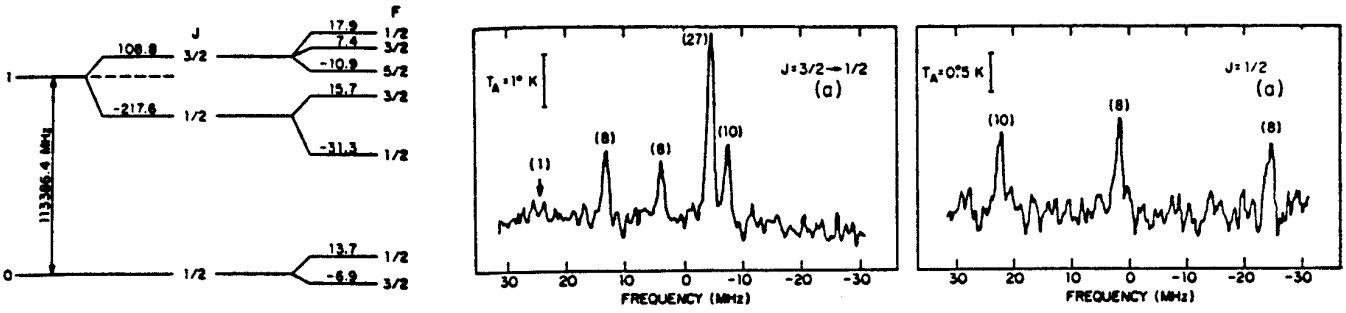

Figure 8.9– CN energy level diagram and measured spectrum toward Orion. The numbers in parenthesis indicate the expected relative strengths of the lines (from Turner and Gammon 1975).

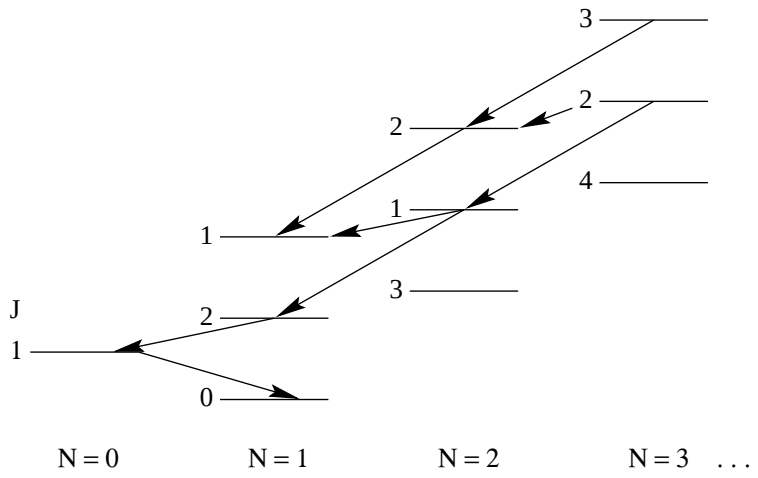

Figure 8.10– SO rotational transitions.

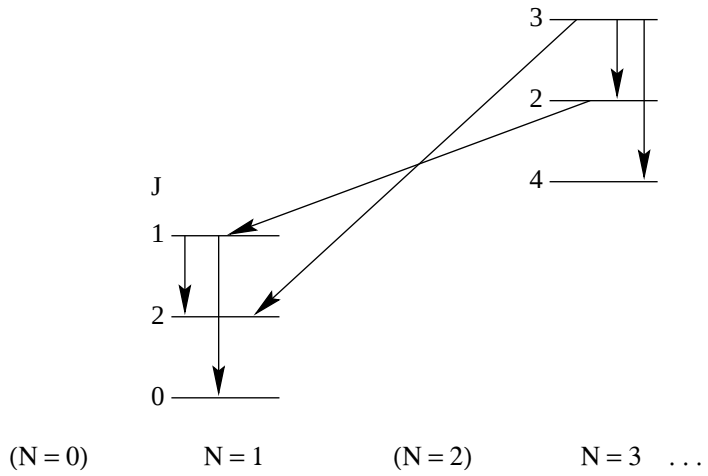

Figure 8.11– $^{16}O_2$ rotational transitions.

e) Examples:

The spectrum of the simplest case of a $^1\Sigma^+$ molecule such as CO has been discussed already above. Briefly, only ΔJ=1 transitions are possible at transition frequencies $\tilde{\nu} = F(J+1) - F(J)$. For CO, B=1.931 cm^{-1}, so that the $J = 1 \rightarrow J = 0$ transition occurs at $\tilde{\nu}$=3.862 cm^{-1} or $\nu = c\tilde{\nu}$ = 115.8 GHz or λ=2.6 mm. Higher transitions are shifted to shorter wavelengths; for example the $J = 16 \rightarrow$15 transition occurs at 163 μm. (See Figure 8.6.)

A more complicated case is provided by the SO molecule, for which the electronic ground state is X $^3\Sigma^-$. The energy levels can be classified according to Hund's case b, and are illustrated, in a slightly different way as before, in Figure 8.10. Possible transitions with ΔJ=1 and 0 are indicated. The approximate selection rule $\Delta N \neq 0$ holds to a high degree in this case.

The electronic ground state of $^{16}O_2$ also has X $^3\Sigma_g^-$ symmetry, but as we have seen, only odd levels can occur in this case. The energy level structure is shown in Figure 8.11. The transitions are electric dipole forbidden, but ΔN=0 transitions can occur according to

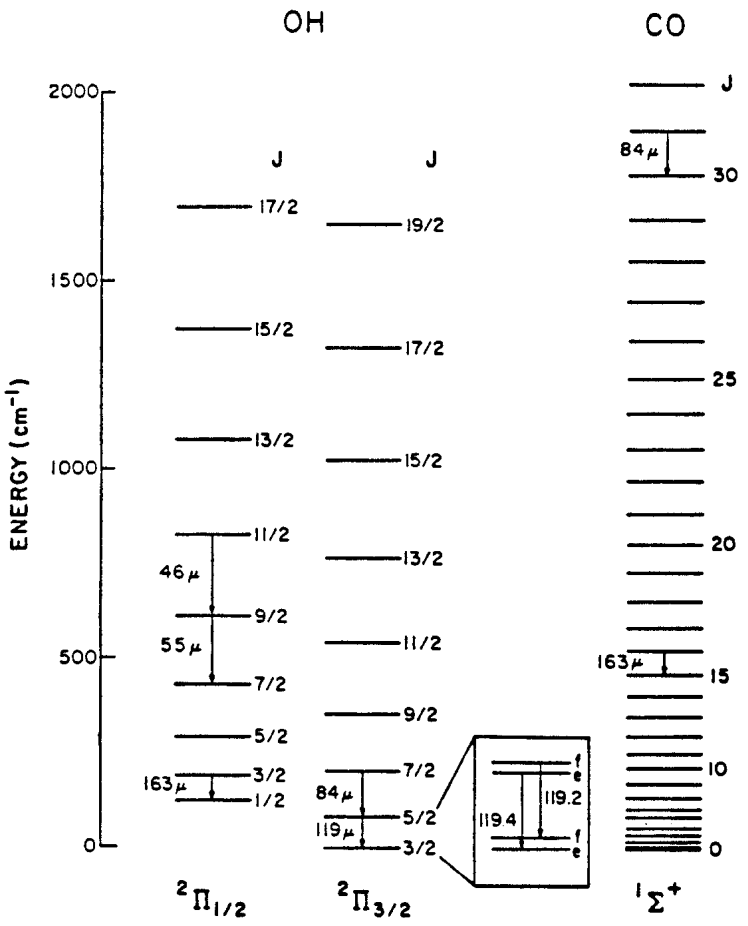

Figure 8.12– A comparison of the OH and CO rotational ladders.

magnetic dipole selection rules, as can ΔN=2 transitions with $\Delta J = \pm 1$. These transitions occur in the microwave region. In the $^{16}O^{18}O$ species, nuclear spin symmetry no longer excludes the N=even levels. Thus, there will be transitions N=even$\rightarrow$ $N-2$ =even that have no counterparts in the $^{16}O_2$ spectrum. This can be useful if one is trying to see astronomical sources of O_2 through the strong atmospheric absorption at the $^{16}O_2$ transition frequency (see, for example, Black and Smith 1984, *Ap. J.* **277**, 562).

The energy level structure of a $^2\Pi$ molecule such as OH is shown in Figure 8.12, and in more detail in the bottom part of Figure 8.13. Figure 8.12 clearly shows the individual rotational ladders in the $^2\Pi_{1/2}$ and $^2\Pi_{3/2}$ states. Each rotational level J is split due to Λ-doubling into a so-called e and f component, which have different parity (see inset Figure 8.12). For the lowest-lying level $^2\Pi_{3/2}, J = 3/2$, this splitting is about 0.055 cm^{-1}. The insert of Figure 8.13 shows the details of the ground state Λ-doublet, which is further split by hydrogen hyperfine structure into a total of 4 levels labelled by $\vec{F} = \vec{J} + \vec{I}$ and parity. There are four possible microwave transitions between these levels, and their frequencies are given. These transitions, which occur around 18 cm, are widely observed from interstellar, circumstellar and cometary OH molecules.

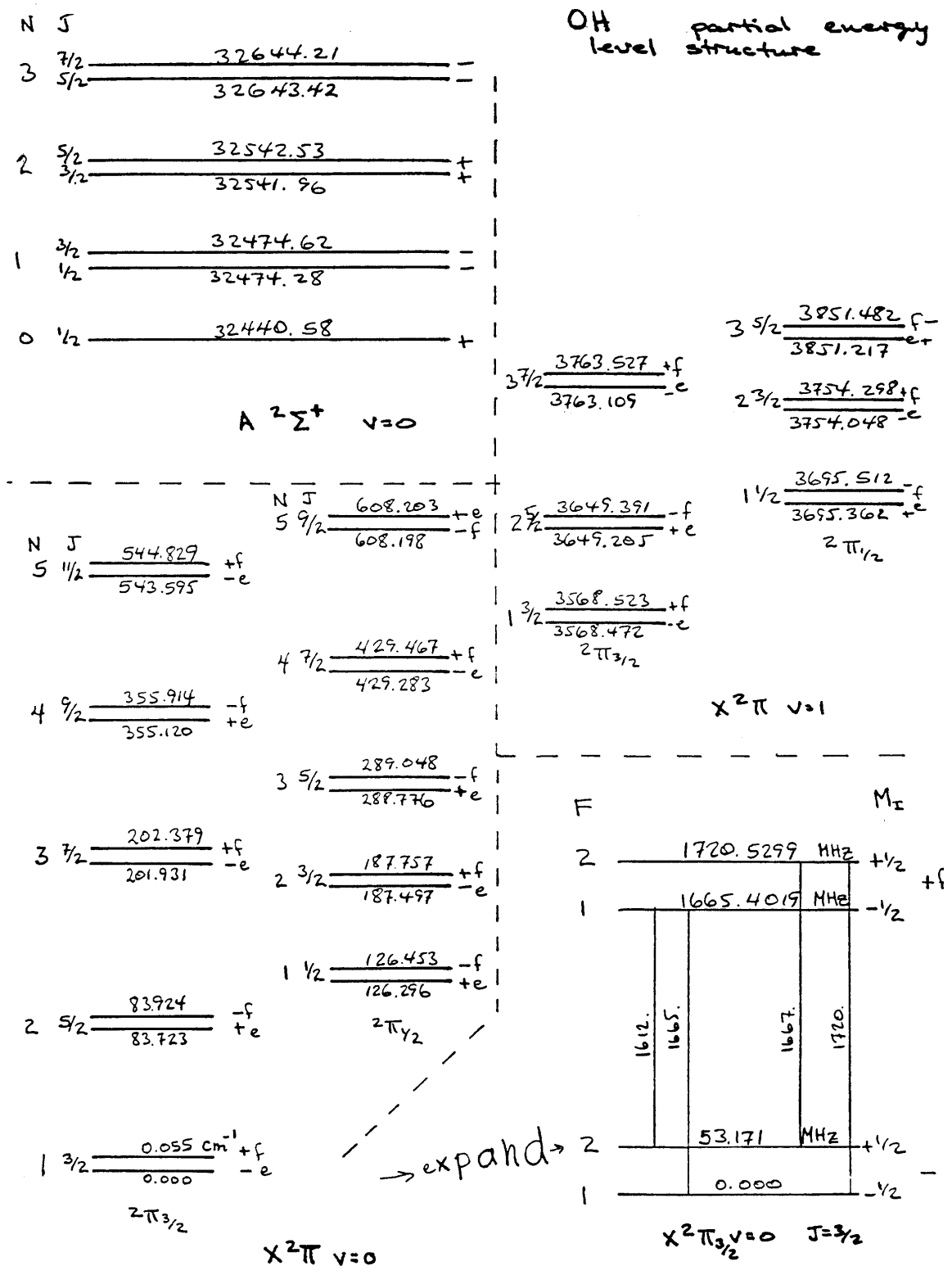

Figure 8.13– A detailed overview of the lowest rotational levels in the X $^2\Pi$ and A $^2\Sigma$ electronic states of the hydroxyl radical.

Note that the rotational constants of diatomics having two heavy nuclei are $B \approx$1-5 cm^{-1} so that their transitions occur at millimeter wavelengths. The rotational constants for hydrides such as CH, NH, OH, etc... are typically $B \approx$10-20 cm^{-1}, so that their lowest lying pure rotation transitions occur at 'submillimeter' wavelengths (0.1-1 mm; 300-3000 GHz). It is only very recently that sub-millimeter telescopes located at high elevations, such as the Caltech Submillimeter Observatory (CSO) and the British-Dutch-Canadian James Clerk Maxwell Telescope (JCMT) atop Mauna Kea, are becoming available to search for these molecules in dense clouds.

3. Symmetric top molecules

In general, the rotational Hamiltonian can be written as

$$H^{rot} = \frac{1}{2}\left(\frac{J_a^2}{I_a} + \frac{J_b^2}{I_b} + \frac{J_c^2}{I_c}\right) \tag{8.29}$$

where $J^2 = J_A^2 + J_b^2 + J_c^2$. For a prolate top, $I_b = I_c$, so we can write

$$H^{rot} = \frac{1}{2}\left(\frac{J^2}{I_b} - \frac{J_a^2}{I_b} - \frac{J_c^2}{I_b} + \frac{J_a^2}{I_a} + \frac{J_c^2}{I_c}\right) \tag{8.30a}$$

or

$$H^{rot} = \frac{1}{2}\left(\frac{J^2}{I_b} + \frac{J_a^2}{I_b} + \frac{J_a^2}{I_a}\right). \tag{8.30b}$$

We know that $J^2 Y_{JM} = J(J+1)Y_{JM}$. Any one of the components corresponding to angular momentum along one of the principal axes is quantized in units of K, with energy proportional to K^2. For example, for a prolate top like CH_3I, J_a represents the angular momentum due to motion about the a-axis, see Figure 8.14.

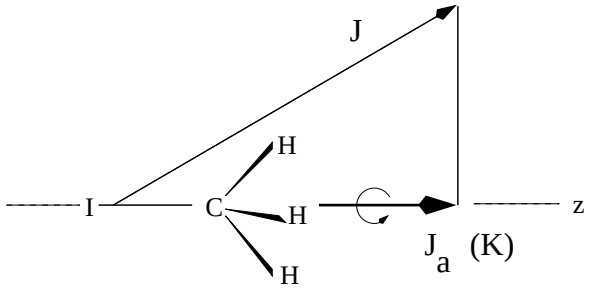

Figure 8.14– J, K (J_a) definitions for a prolate top.

Thus, we find for a prolate top:

$$E^{rot} = \frac{J(J+1)}{2I_b} + \frac{K^2}{2}\left(\frac{1}{I_a} - \frac{1}{I_b}\right) \tag{8.31}$$

$$= BJ(J+1) + (A-B)K^2.$$

For an oblate top, we use similar steps to obtain:

$$E^{rot} = BJ(J+1) + (C-B)K^2. \tag{8.32}$$

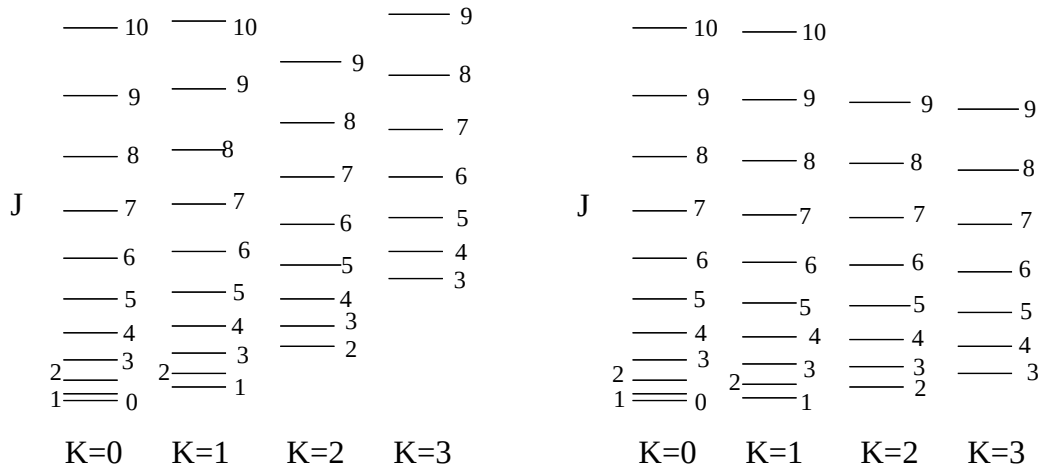

Figure 8.15– Rotational energy levels for (a) a prolate and (b) an oblate symmetric top.

The quantum number K can take values $K = 0, 1, 2, ...J$ where all levels for $K > 0$ are doubly degenerate due to the equivalency of clockwise and anticlockwise rotation. For the linear rotor, which is special case of a symmetric top, $K = \Lambda$. Thus, each J level then has the usual $2J + 1$ different K states, corresponding to the different possible projections of J on a 'molecule-fixed' axis. Each (J, K) level then has $2J + 1$ different M_J levels, corresponding to the different possible projections of J on a 'space-fixed' axis. Thus, the statistical weight for each J level is $(2J + 1)^2$, rather than the $2J + 1$ we saw for a linear (or diatomic) rotor. Figure 8.15 illustrates the energy levels for a prolate and an oblate top. Since $A > B > C$, the energy of a certain J level increases with K for a prolate top, but decreases with K for an oblate top.

The selection rules for symmetric tops are

$$\Delta J = \pm 1, \Delta K = 0, \tag{8.33}$$

in addition to the requirement that the molecule must have a permanent dipole moment. Thus, transitions between the various K-ladders are forbidden. The $\Delta K = 0$ rule also results in a simple expression for the transition frequencies

$$\nu = F(J + 1, K) - F(J, K) = 2B(J + 1) \tag{8.34}$$

which is the same for a diatomic or linear polyatomic molecule.

When the effects of centrifugal distortion are included, the term values for a prolate symmetric top in a non-degenerate vibrational level of a non-degenerate singlet electronic state becomes

$$F_v(J, K) = B_v J(J+1) + (A_v - B_v)K^2 - D_K K^4 - D_{JK} J(J+1)K^2 - D_J J^2(J+1)^2 \tag{8.35}$$

where there are now three distortion constants D_J, D_{JK} and D_K. An analogous expression holds for an oblate symmetric rotor.

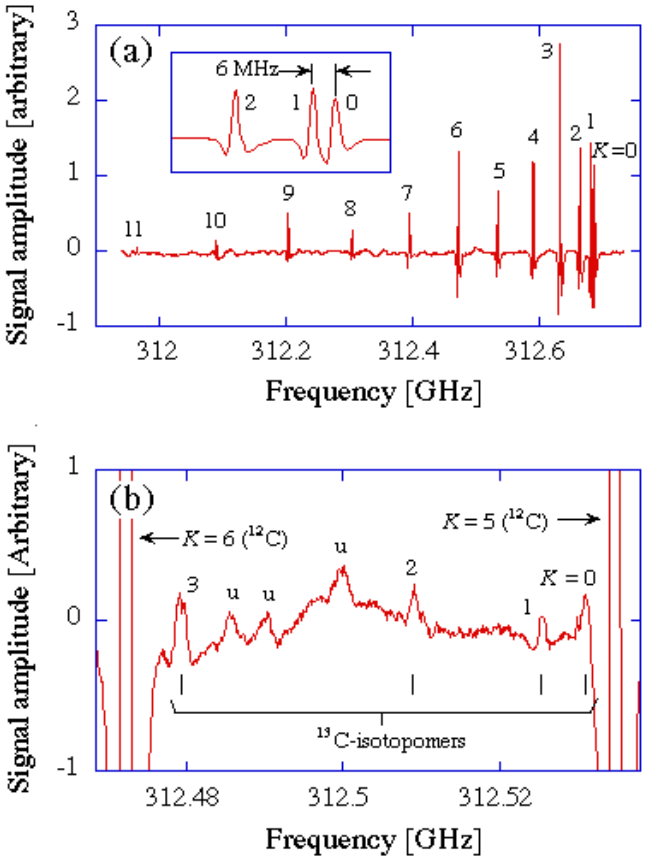

Figure 8.16– The rotational spectrum of acetonitrile near 312 GHz. The small features in the lower panel are from the $CH_3{}^{13}CN$ isotopomer of acetonitrile. Rotational constants from a suite of isotopomers can be used to determine the structure of the molecule to high precision since the moments of inertia depend on the masses and bond lengths involved.

When the $\Delta J = 0, \pm 1$ and $\Delta K = 0$ electric dipole selection rules are used, the frequency expression for the rotational transitions in a prolate top becomes

$$\nu(J,K) = 2(B_v - D_{JK}K^2)(J+1) \; - \; 4D_J(J+1)^3 \tag{8.36}$$

Notice that the pure rotational spectrum does not contain any information about A_v or D_K. It turns out vibrational spectroscopy must be used to determine these constants, or very weakly allowed $\Delta K = \pm 3$ pure rotational transitions must be sought out. The latter are analogous to the spherical top pure rotational spectrum shown at the end of Lecture #8. Again, an analogous expression holds for an oblate symmetric rotor.

The spectrum in Figure 8.16 is for the $J = 16_K \rightarrow 17_K$ stack of acetontrile, CH_3CN, near 312 GHz. The K^2 nature of the JK interaction is clearly visible. From spectra such as this alone it is possible to fit the D_{JK} term, fits of B_v and D_J require the measurement of several different bands with different values of J.

While the A rotational constant cannot be determined directly from the rotational spectra of prolate symmetric tops, it does have a major impact on the appearance of

the spectrum. Since the rotational energies depend strongly on (A-B), in a gas under thermal equilibrium conditions the relative intensities of the various K components will be a sensitive function of the ambient temperature. Unlike diatomic or linear molecules, however, one need not measure many lines over a wide frequency range in order to constrain the temperature – the small effects of centrifugal distortion split the temperature sensitive states sufficiently far in order to allow temperature measurements to be made, but not so far that many different instruments need be used. Thus, symmetric tops are very handy thermometers in astrophysics and planetary science.

Nuclear spin statistics can also influence the weights of the various rotational levels of a polyatomic molecule, but the formulae for calculating these are somewhat complicated. Qualitatively, the effects for symmetric tops with three equivalent hydrogens are easy to see in Figure 8.16 in the $K = 3, 6, 9$ components. In this case the three hydrogens lead to two different overall spin symmetries labeled A and E, with relative spin weights $E : A = 2 : 1$. The E states correlate with $K = 0, 3, 6, 9, 12, 15, ...$, the A states are the remainder. When fitting temperatures to the overall rotational manifolds it is important to keep these effects in mind. See Herzberg vol. II for more details.

The most important astrophysical example of a symmetric top molecule is ammonia, NH_3. However, we will postpone discussion of its spectrum until § IX.

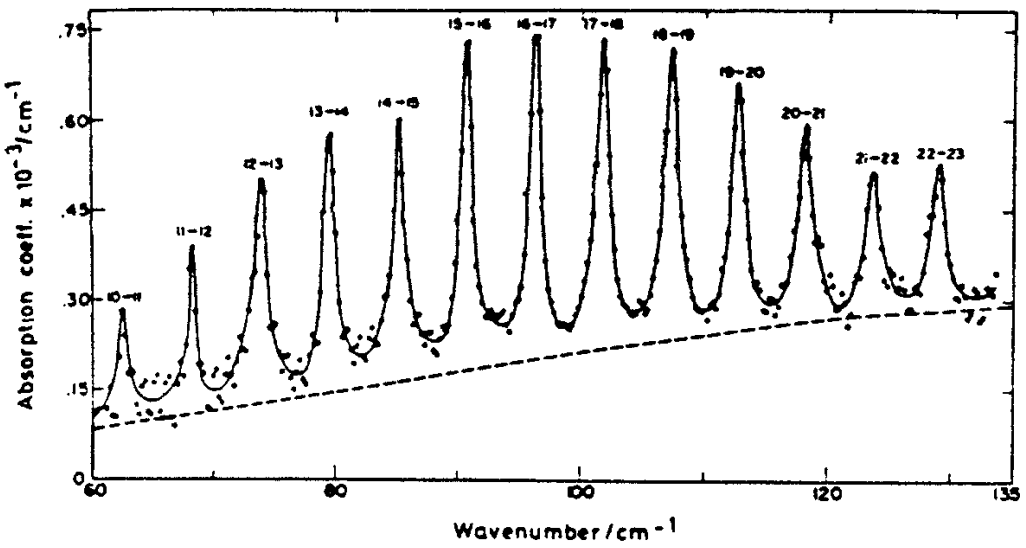

Figure 8.17- Far-infrared pure rotational spectrum of the silane (SiH_4) spherical top.

4. Spherical top molecules.

Using similar arguments as for prolate tops, we find from Equation (8.29) with $I_a = I_b = I_c$ that

$$E^{rot} = BJ(J+1). \tag{8.37}$$

In the absence of vibration-rotation interactions, all $(2J+1)^2$ levels are degenerate. The selection rule is again $\Delta J = \pm 1$.

The spherical top molecule of prime astrophysical importance is CH_4. Since the molecule has no permanent dipole moment, one would not expect it to have a millimeter

(rotational) spectrum. However, rotation about any of the four axes containing a C-H bond results in a 'centrifugal distortion' in which the other 3 hydrogen atoms are thrown outwards slightly from the axis. This converts the molecule into a symmetric rotor and gives it a small dipole moment, 10^{-6} D, resulting in a very weak rotational spectrum. Part of the far-infrared ($\lambda \approx 10 - 100$ μm) spectrum of the analogous molecule SiH_4 is shown in Figure 8.17. It has the same regular spacing as the spectrum of a linear rotor.

5. Asymmetric top molecules

Most molecules are asymmetric tops with $I_a \neq I_b \neq I_c$. Thus, the rotational Hamiltonian

$$H^{rot} = \frac{1}{2}\left(\frac{J_a^2}{I_a} + \frac{J_b^2}{I_b} + \frac{J_c^2}{I_c}\right) \tag{8.38}$$

cannot be factored as it was for symmetric and spherical tops. Hence, no simple energy expression can be written for this general case, especially when centrifugal distortion is include. Some approximate energy level expressions for low J can be calculated assuming a rigid rotor model, and are listed in Table 8.4 for $J < 4$. Computer programs are available to calculate the asymmetric rotor energy levels in general.

Table 8.4 – Asymmetric Top Rotational Energies

$J_{K_pK_o}$	Rotational Energy
0_{00}	0
1_{01}	$B + C$
1_{11}	$A + C$
1_{10}	$A + B$
2_{02}	$2A + 2B + 2C \; - \; 2\sqrt{(B-C)^2 + (A-C)(A-B)}$
2_{12}	$A + B + 4C$
2_{11}	$A + 4B + C$
2_{21}	$4A + B + C$
2_{20}	$2A + 2B + 2C \; + \; 2\sqrt{(B-C)^2 + (A-C)(A-B)}$
3_{03}	$2A + 5B + 5C \; - \; 2\sqrt{4(B-C)^2 + (A-B)(A-C)}$
3_{13}	$5A + 2B + 5C \; - \; 2\sqrt{4(A-C)^2 - (A-B)(B-C)}$
3_{12}	$5A + 5B + 2C \; - \; 2\sqrt{4(A-B)^2 + (A-C)(B-C)}$
3_{22}	$4A + 4B + 4C$
3_{21}	$2A + 5B + 5C \; + \; 2\sqrt{4(B-C)^2 + (A-B)(A-C)}$
3_{31}	$5A + 2B + 5C \; + \; 2\sqrt{4(A-C)^2 - (A-B)(B-C)}$
3_{30}	$5A + 5B + 2C \; + \; 2\sqrt{4(A-B)^2 + (A-C)(B-C)}$

Given the three rotational constants, an asymmetric rotor can be characterized by a parameter

$$\kappa = \frac{2B - A - C}{A - C} \tag{8.39}$$

which can take on values between +1 and –1. If κ is near –1, then the rotor is 'near-prolate', and Equation (8.30), with a nearly good quantum number K_p, is applicable; the

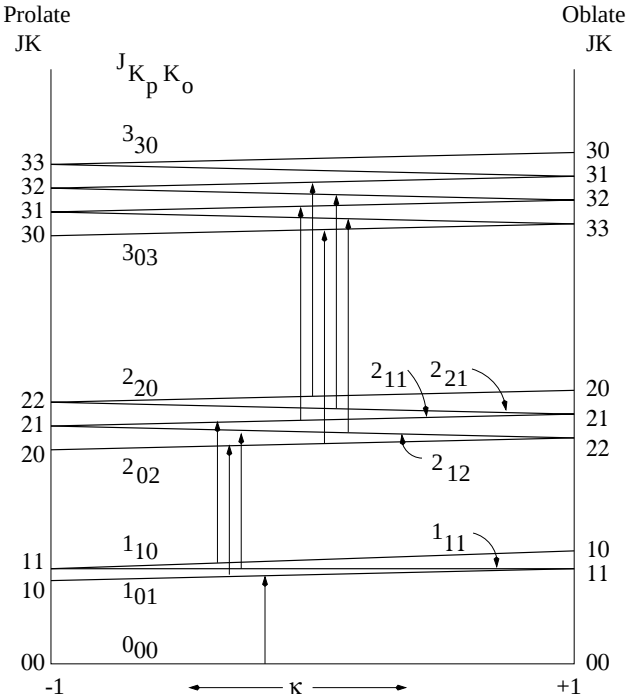

Figure 8.18– Energy levels for $J = 0, 1, 2, 3$ of the asymmetric rotor. This correlation diagram is qualitative in nature, and does not accurately represent the true level spacings. The value of $\kappa = (2B-A-C)/(A-C)$ runs from -1 (the prolate top limit) to +1 (the oblate top limit). Also indicated are the electric dipole allowed transitions for a near-prolate rotor such as formaldehyde or propynal, subject to selection rules $\Delta K_p = 0$, $\Delta K_o = \pm 1$.

small asymmetry produces a splitting of the energy levels with $K_p > 0$. Similarly, if κ is near +1, then the rotor is 'near-oblate' and we can use Equation (8.32) with a quantum number K_o. Again, there will be an asymmetry doubling for $K_o > 0$. The rotation states are labelled as

$$J_{K_p K_o} \tag{8.40}$$

where K_p and K_o are the K values that the molecule would have in the limiting oblate and prolate cases, respectively. Sometimes, the notation $J_{K_a K_c}$ or $J_{K_{-1} K_{+1}}$ is used. A correlation diagram showing how these energy expressions vary between the prolate and oblate limits is shown in Figure 8.18.

A more thorough discussion of all of these matters, as well as tables for the energy level expressions can be found in Townes and Schawlow, "Microwave Spectroscopy," or Gordy and Cook, "Microwave Molecular Spectra."

The selection rule $\Delta J = 0, \pm 1$ still applies for asymmetric top molecules, and the molecule must have a permanent dipole moment. In general, the dipole moment may have non-vanishing components along more than one of the principal axes; thus an asymmetric top can have two different 'types' of rotational transitions, often at quite different frequencies. The closer a molecule is to one of the limiting cases, the better it will obey the selection rules for symmetric tops. In some near-prolate tops, it is even possible to find two kinds of selection rules, namely, $\Delta K_p = 0$ and $\Delta K_o = \pm 1$.

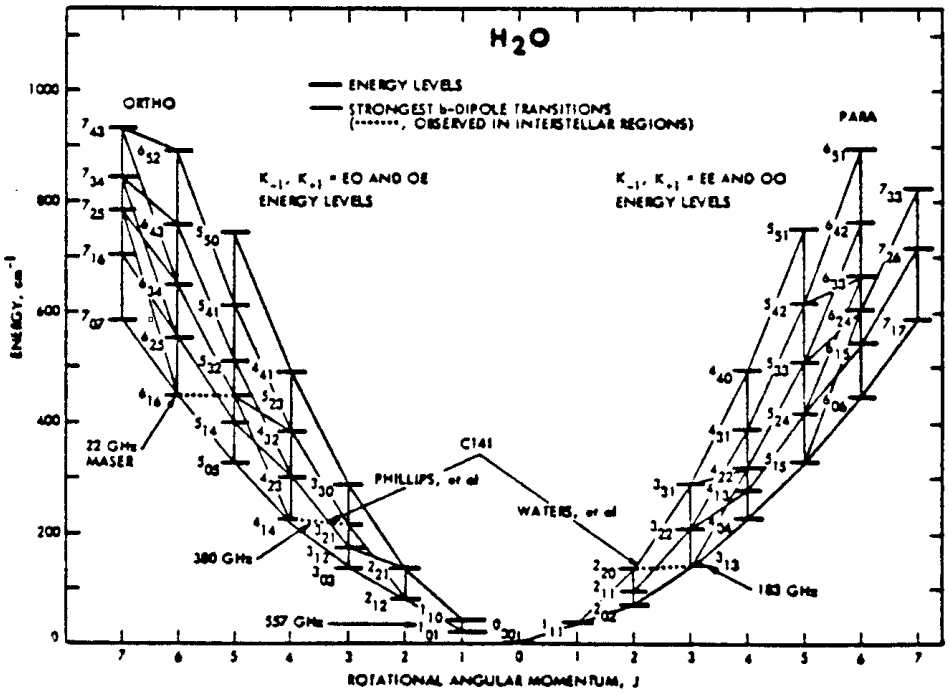

Figure 8.19– Rotational energy levels for water, with some of the astrophysically-detected transitions marked.

One of the most important astrophysical examples of an asymmetric rotor is the H_2O molecule, whose energy level diagram is reproduced in Figure 8.19. The molecule has two equivalent H nuclei, giving rise to *ortho*-H_2O and *para*-H_2O. The lowest level of the molecule, 0_{00}, belongs to the *para*-version. The lowest level of the *ortho*-form is 1_{01}. These two forms cannot be interconverted except in collisions in which a H nucleus is exchanged.

The lowest lying transitions with $\Delta J = 1$ or $\Delta K = 1$ all lie at submillimeter and far-infrared wavelengths. For example, the lowest *para* transition $1_{11} - 0_{00}$ occurs at 269 μm (1113 GHz), and the lowest *ortho* transition $1_{10} - 1_{01}$ at 539 μm (557 GHz). Because of the water in the Earth's atmosphere, these lines cannot be observed using ground based telescopes, and have therefore not been detected in interstellar clouds. Some higher-lying transitions have been observed from the Kuiper Airborne Observatory (KAO) in warm regions, but it is difficult to derive abundances from them. As a consequence, the abundance of H_2O in dense interstellar clouds is one of the major uncertainties in their chemistry. The ISO satellite has made a large number of measurements in the far-infrared, but cannot resolve the line profiles; while the heterodyne-receiver based SWAS has made very high spectral resolution measurements of the lowest ortho transition. A very famous transition in H_2O is the $6_{16} - 5_{23}$ transition in the *ortho*-ladder, which occurs at 22 GHz. This line shows strong 'maser' emission near star-forming regions.

Another interesting astrophysical example is C_3H_2, cyclopropeniylidene, which is the first ring molecule detected in interstellar clouds (Thaddeus *et al.* 1985, *Ap. J. Letters* **299**, L63). Its energy level structure is illustrated in Figure 8.20, while Figure 8.21 shows some of the observed lines in the Taurus molecular clouds. Some of the lines occur in emission, others in absorption.

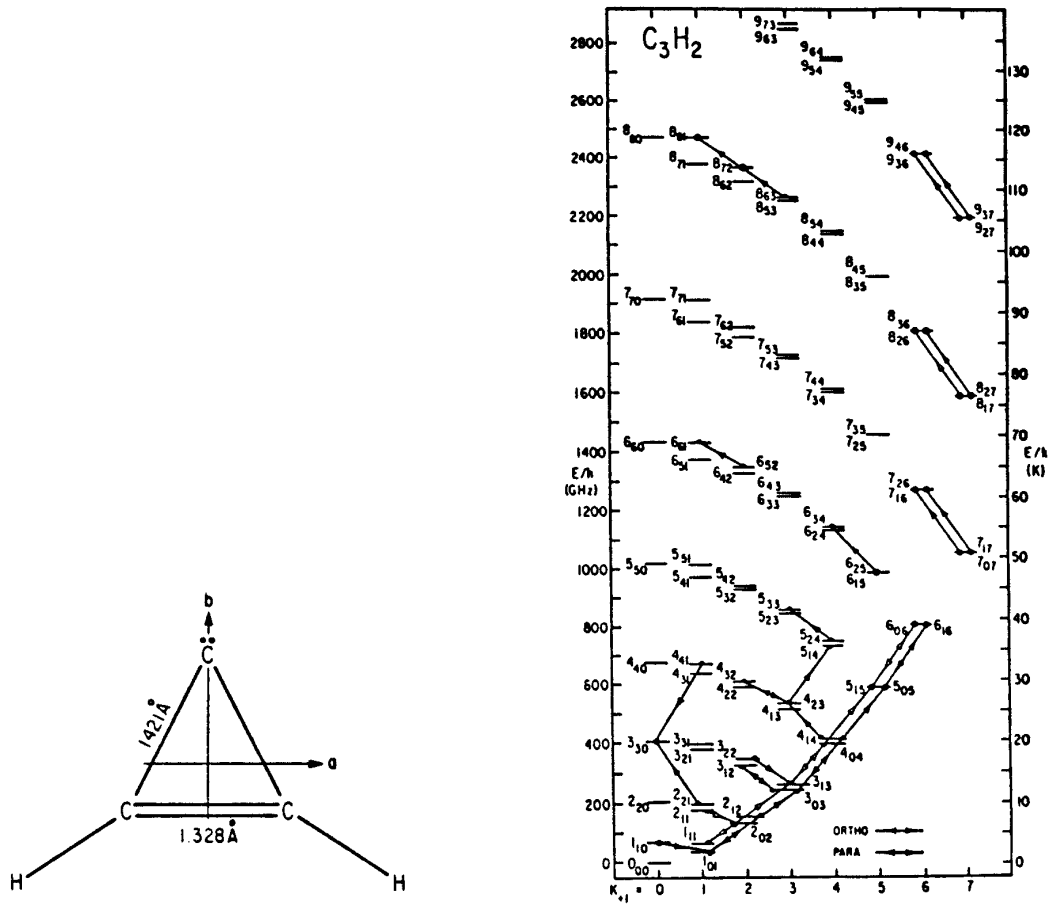

Figure 8.20– Rotational levels of C_3H_2 (structure at left). Downward arrows indicate astronomically observed transitions, mainly in emission. Upward ones indicate transitions observed in the laboratory.

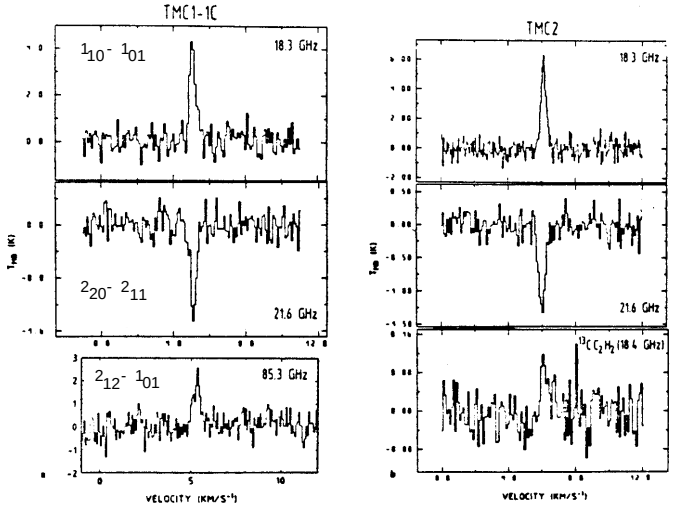

Figure 8.21– C_3H_2 rotational lines observed toward the cold, dark cloud Taurus Molecular Cloud 1 (TMC1).